Max-Planck-Institut für Mathematik in den Naturwissenschaften Leipzig

Tucker tensor method for fast grid-based summation of long-range potentials on 3D lattices with defects

(revised version: October 2014)

by

Venera Khoromskaia and Boris N. Khoromskij

Preprint no.: 88 2014

Tucker tensor method for fast grid-based summation of long-range potentials on 3D lattices with defects

Venera Khoromskaia* Boris N. Khoromskij**

Abstract

We introduce the Tucker tensor method for the grid-based assembled summation of long-range interaction potentials over large 3D lattices in a box. This method is a generalization of our previous approach on the low-rank canonical tensor summation of electrostatic potentials on a rectangular 3D lattice. In the new technique we first approximate (with a guaranteed precision) the single kernel function represented on large $N \times N \times N$ 3D grid in a bounding box by a low-rank reference Tucker tensor. Then each 3D singular kernel function involved in the summation is approximated on the same grid by the shift of the reference Tucker tensor. Directional vectors of the Tucker tensor representing a full lattice sum are assembled by the 1D summation of the corresponding Tucker vectors for shifted potentials, while the core tensor remains unchanged. The Tucker ranks of the resultant tensor sum on the 3D rectangular $L \times L \times L$ lattice are proven to be the same as for the single kernel function. The required storage scales linearly in the 1D grid-size, $O(N)$, while the numerical cost is estimated by $O(NL)$. With the slight modifications our approach applies in the presence of defects, such as vacancies, impurities and non-rectangular geometries of a set of active lattice points, as well as for the case of hexagonal lattices. For potential sums with defects the Tucker rank of the resultant tensor may increase, so that we apply the ε-rank truncation procedure based on the generalized reduced HOSVD approximation combined with the ALS iteration. We prove the error bounds and stability for the HOSVD Tucker approximation to a sum of canonical/Tucker tensors. Numerical tests confirm the efficiency of the presented tensor summation method. In particular, we show that a sum of millions of Newton kernels on a 3D lattice with defects/impurities can be computed in about a minute in Matlab implementation. The approach is beneficial for functional calculus with the lattice potential sum represented on large 3D grids in the Tucker/canonical formats. Indeed, the interpolation, scalar product with a function, integration or differentiation can be performed easily in tensor arithmetics with 1D complexity.

AMS Subject Classification: 65F30, 65F50, 65N35, 65F10
Key words: Lattice sums, canonical tensor format, Tucker tensor decomposition, lattice in a box, lattice defects, long-range potentials, classical interaction potentials, tensor numerical methods, electronic structure calculations.

*Max-Planck-Institute for Mathematics in the Sciences, Inselstr. 22-26, D-04103 Leipzig, Germany (vekh@mis.mpg.de).

**Max-Planck-Institute for Mathematics in the Sciences, Inselstr. 22-26, D-04103 Leipzig, Germany (bokh@mis.mpg.de).

1 Introduction

Summation of classical long-range potentials on a 3D lattice, or, more generally, of arbitrarily distributed potentials in a volume, is one of the challenges in the numerical treatment of many-body systems in molecular dynamics, quantum chemical computations, simulations of large solvated biological systems and other applications, see for example [43, 36, 6, 37, 14, 38], [42, 21, 10], and [12]. Beginning with the widely spread Ewald summation techniques [15], the development of lattice-sum methods has led to well established algorithms for numerical evaluation of long-range interaction potentials of large multiparticle systems, see for example [8, 40, 42, 21, 10] and references therein. The numerical complexity of the respective computational schemes scales at least linearly in the full volume size of the lattice. These methods usually combine the original Ewald summation approach with the fast Fourier transform (FFT) or fast multipole methods [18]. The fast multipole method is widely used for summation of non-uniformly distributed potentials, that combines direct approximation of closely positioned potentials and clustered summation of far fields.

The new generation of grid-based lattice summation techniques applied to long-range interaction potentials on a rectangular 3D lattices is based on the idea of assembled directional summation in the low-rank canonical tensor format [25]. This approach allows the efficient treatment of large 3D sums with linear complexity scaling in the 1D lattice-size.

In this paper, we introduce the new and more general Tucker tensor method for the grid-based assembled summation of classical potentials on 3D lattices in a box, which remains efficient in the presence of vacations, impurities and in the case of some non-rectangular lattices. In particular, it is applicable to the calculation of electrostatic potential in the case of non-rectangular geometry of the active set of lattice points with multilevel step-type boundaries with holes, etc., see §5.

In the new approach, we first approximate (with a guaranteed precision) the single kernel function represented on large $N \times N \times N$ 3D grid in a bounding box by a low-rank reference Tucker tensor. This tensor provides the values of the discretized potential at any point of the fine $N \times N \times N$ grid, but needs only $O(N)$ storage in both the canonical and Tucker tensor formats. Then each 3D singular kernel function involved in the summation is approximated on the same grid by a shift of the reference Tucker tensor. Directional vectors of the Tucker tensor representing a full lattice sum are assembled by the 1D summation of the corresponding Tucker vectors for shifted potentials, while the core tensor remains unchanged. The Tucker ranks of the resultant tensor sum on the 3D rectangular $L \times L \times L$ lattice are proven to be the same as for the single kernel function. The required storage scales linearly in the 1D grid-size, $O(N)$, while the numerical cost is estimated by $O(NL)$. Though the lattice nodes are not required to exactly coincide with the grid points of the global $N \times N \times N$ grid, the resulting accuracy of the representation is nevertheless well controlled due to easy availability of large grid size N.

The formatted tensor approximation of the spherically symmetric reference potential is based on the low-rank representation of the analytic kernel functions by using the integral Laplace transform and its quadrature approximation. In particular, the algorithm based on the *sinc*-quadrature approximation to the Laplace transform of the Newton kernel function $\frac{1}{r}$ developed in [1] (see also [5, 19, 16]), can be adapted. Literature surveys addressing the most commonly used in computational practice tensor formats like canonical, Tucker and matrix

product states (or tensor train) representations, as well as basics of multilinear algebra and the recent tensor numerical methods for solving PDEs, can be found in [34, 32, 17, 33] (see also Dissertations [22] and [11]).

The presented approach yields enormous reduction in storage and computing time. Our numerical results show that summation of two millions of potentials on a 3D lattice on a grid of size 10^{15} takes about 15 seconds in Matlab implementation. Similar to the case of canonical decompositions, ranks of the resulting Tucker tensor representing the total sum of a large number of potentials remains the same as for the Tucker tensor representation of a single potential. This concept was boiled up based on numerical tests in [30, 22], where it was observed that the Tucker tensor rank of the 3D lattice sum of discretized Slater functions is close to the rank of a single Slater function.

In the case of sums with defects, we generalize the reduced HOSVD (RHOSVD) rank reduction scheme applied to the canonical format [31] (see [9] concerning the notion of HOSVD scheme) to the cases of Tucker input tensors. The RHOSVD scheme was applied, in particular, to the *direct* summation of the electrostatic potentials of nuclei in a molecule [23] for calculation of the one-electron integrals in the framework of 3D grid-based Hartree-Fock solver by tensor-structured methods [24]. In general, the direct summation of canonical/Tucker tensors with RHOSVD-type rank reduction proves to be efficient in the case of rather arbitrary positions of a moderate number of potentials (like nuclei in a single molecule).

Notice that the canonical/Tucker tensor representation of the lattice sum of interaction potentials can be computed with high accuracy, and in a completely algebraic way. In the presence of defects, the rank bounds for the tensor representation of a sum of potentials can be easily estimated. The grid-based tensor approach is beneficial in applications requiring further functional calculus with the lattice potential sums, for example, interpolation, scalar product with a function, integration or differentiation (computation of energies or forces), which can be performed on large 3D grids using tensor arithmetics of sub-linear cost [22, 31]. The summation cost in the Tucker/canonical formats, $O(L\,N)$, can be reduced to the logarithmic scale in the lattice size, $O(L \log N)$, by using the low-rank quantized tensor approximation (QTT), see [29], of long canonical/Tucker vectors as suggested and analyzed in [25].

The rest of the paper is structured as following. §2 discusses the rank bounds for 3D grid-based canonical/Tucker tensor representations to a single kernel based on the general approximation properties of tensor decompositions to a class of analytic kernel functions. Section §3 describes the idea of the direct calculation of a sum of the shifted single potentials on a lattice focusing on the main topic of the paper, the construction and analysis of the algorithms of assembled Tucker tensor summation of the non-local potentials on a rectangular 3D lattice. §4 generalizes the Tucker representation with the rank optimization to 3D lattice sums with defects, while §5 outlines the extension of the tensor-based lattice summation techniques to the class of non-rectangular lattices or rather general shape of the set of active lattice points (say, multilevel step-type boundaries).

2 Tensor decomposition for analytic potentials

2.1 Grid-based canonical/Tucker representation of a single kernel

Methods of separable approximation to the 3D Newton kernel (electrostatic potential) using the Gaussian sums have been addressed in the chemical and mathematical literature since [3] and [4, 5], respectively.

In this section, we discuss the grid-based method for the low-rank canonical and Tucker tensor representations of a spherically symmetric kernel function $p(\|x\|)$, $x \in \mathbb{R}^d$ for $d = 1, 2, 3$ (for example, for the 3D Newton we have $p(\|x\|) = \frac{1}{\|x\|}$, $x \in \mathbb{R}^3$) by its projection onto the set of piecewise constant basis functions, see [1] for more details. For the readers convenience, we now recall the main ingredients of this tensor approximation scheme.

In the computational domain $\Omega = [-b/2, b/2]^3$, let us introduce the uniform $n \times n \times n$ rectangular Cartesian grid Ω_n with the mesh size $h = b/n$. Let $\{\psi_{\mathbf{i}}\}$ be a set of tensor-product piecewise constant basis functions, $\psi_{\mathbf{i}}(\mathbf{x}) = \prod_{\ell=1}^{d} \psi_{i_\ell}^{(\ell)}(x_\ell)$, for the 3-tuple index $\mathbf{i} = (i_1, i_2, i_3)$, $i_\ell \in \{1, ..., n\}$, $\ell = 1, 2, 3$. The kernel $p(\|x\|)$ can be discretized by its projection onto the basis set $\{\psi_{\mathbf{i}}\}$ in the form of a third order tensor of size $n \times n \times n$, defined point-wise as

$$\mathbf{P} := [p_{\mathbf{i}}] \in \mathbb{R}^{n \times n \times n}, \quad p_{\mathbf{i}} = \int_{\mathbb{R}^3} \psi_{\mathbf{i}}(x) p(\|x\|)\, \mathrm{d}x. \tag{2.1}$$

The low-rank canonical decomposition of the 3rd order tensor $\mathbf{P}$ is based on using exponentially convergent sinc-quadratures for approximation of the Laplace-Gauss transform to the analytic function $p(z)$ specified by certain weight $a(t) > 0$,

$$p(z) = \int_{\mathbb{R}_+} a(t) e^{-t^2 z^2}\, \mathrm{d}t \approx \sum_{k=-M}^{M} a_k e^{-t_k^2 z^2} \quad \text{for} \quad |z| > 0, \tag{2.2}$$

where the quadrature points and weights are given by

$$t_k = k\mathfrak{h}_M, \quad a_k = a(t_k)\mathfrak{h}_M, \quad \mathfrak{h}_M = C_0 \log(M)/M, \quad C_0 > 0. \tag{2.3}$$

Under the assumption $0 < a \le \|z\| < \infty$ this quadrature can be proven to provide the exponential convergence rate in M for a class of analytic functions $p(z)$, see [41, 19, 28]. We proceed with further discussion of this issue in §2.2.

For example, in the particular case $p(z) = 1/z$ we apply the Laplace-Gauss transform

$$\frac{1}{z} = \frac{2}{\sqrt{\pi}} \int_{\mathbb{R}_+} e^{-z^2 t^2} dt,$$

which can be adapted to the Newton kernel by substitution $z = \sqrt{x_1^2 + x_2^2 + x_3^2}$.

Now for any fixed $x = (x_1, x_2, x_3) \in \mathbb{R}^3$, such that $\|x\| > 0$, we apply the sinc-quadrature approximation to obtain the separable expansion

$$p(\|x\|) = \int_{\mathbb{R}_+} a(t) e^{-t^2 \|x\|^2}\, \mathrm{d}t \approx \sum_{k=-M}^{M} a_k e^{-t_k^2 \|x\|^2} = \sum_{k=-M}^{M} a_k \prod_{\ell=1}^{3} e^{-t_k^2 x_\ell^2}. \tag{2.4}$$

Under the assumption $0 < a \le \|x\| \le A < \infty$ this approximation provides the exponential convergence rate in M,

$$\left| p(\|x\|) - \sum_{k=-M}^{M} a_k e^{-t_k^2 \|x\|^2} \right| \le \frac{C}{a}\, e^{-\beta\sqrt{M}}, \quad \text{with some } C, \beta > 0. \tag{2.5}$$

Combining (2.1) and (2.4), and taking into account the separability of the Gaussian basis functions, we arrive at the low-rank approximation to each entry of the tensor $\mathbf{P}$,

$$p_{\mathbf{i}} \approx \sum_{k=-M}^{M} a_k \int_{\mathbb{R}^3} \psi_{\mathbf{i}}(\mathbf{x}) e^{-t_k^2 \|\mathbf{x}\|^2} \mathrm{d}\mathbf{x} = \sum_{k=-M}^{M} a_k \prod_{\ell=1}^{3} \int_{\mathbb{R}} \psi_{i_\ell}^{(\ell)}(x_\ell) e^{-t_k^2 x_\ell^2} \mathrm{d}x_\ell.$$

Define the vector (recall that $a_k > 0$)

$$\mathbf{p}_k^{(\ell)} = a_k^{1/3} \left[b_{i_\ell}^{(\ell)}(t_k) \right]_{i_\ell=1}^{n_\ell} \in \mathbb{R}^{n_\ell} \quad \text{with} \quad b_{i_\ell}^{(\ell)}(t_k) = \int_{\mathbb{R}} \psi_{i_\ell}^{(\ell)}(x_\ell) e^{-t_k^2 x_\ell^2} \mathrm{d}x_\ell,$$

then the 3rd order tensor $\mathbf{P}$ can be approximated by the R-term ($R = 2M + 1$) canonical representation

$$\mathbf{P} \approx \mathbf{P}_R = \sum_{k=-M}^{M} a_k \bigotimes_{\ell=1}^{3} \mathbf{b}^{(\ell)}(t_k) = \sum_{q=1}^{R} \mathbf{p}_q^{(1)} \otimes \mathbf{p}_q^{(2)} \otimes \mathbf{p}_q^{(3)} \in \mathbb{R}^{n \times n \times n}, \tag{2.6}$$

where $R = 2M + 1$. For the given threshold $\varepsilon > 0$, M is chosen as the minimal number such that in the max-norm

$$\|\mathbf{P} - \mathbf{P}_R\| \le \varepsilon \|\mathbf{P}\|.$$

The canonical vectors are renumbered by $k \to q = k + M + 1$, $\mathbf{p}_q^{(\ell)} = \mathbf{p}_k^{(\ell)} \in \mathbb{R}^n$, $\ell = 1, 2, 3$. The canonical tensor $\mathbf{P}_R$ in (2.6) approximates the discretized 3D symmetric kernel function $p(\|x\|)$ ($x \in \Omega$), centered at the origin, such that $\mathbf{p}_q^{(1)} = \mathbf{p}_q^{(2)} = \mathbf{p}_q^{(3)}$ ($q = 1, ..., R$).

In the following we also consider a Tucker approximation of the 3rd order tensor $\mathbf{P}$. Given rank parameters $\mathbf{r} = (r_1, r_2, r_3)$, the set of rank-$\mathbf{r}$ Tucker tensors, $\mathcal{T}_{\mathbf{r},n}$ (the Tucker format) is defined by the following parametrization

$$\mathbf{T} = [t_{i_1 i_2 i_3}] = \sum_{\mathbf{k}=\mathbf{1}}^{\mathbf{r}} b_{\mathbf{k}} \mathbf{t}_{k_1}^{(1)} \otimes \mathbf{t}_{k_2}^{(2)} \otimes \mathbf{t}_{k_3}^{(3)} \equiv \mathbf{B} \times_1 T^{(1)} \times_2 T^{(2)} \times_3 T^{(3)}, \quad i_\ell \in \{1, ..., n\},$$

where the side-matrices $T^{(\ell)} = [\mathbf{t}_1^{(\ell)} ... \mathbf{t}_{r_\ell}^{(\ell)}] \in \mathbb{R}^{n \times r_\ell}$, $\ell = 1, 2, 3$, defining the set of Tucker vectors, can be assumed orthogonal. Here $\mathbf{B} \in \mathbb{R}^{r_1 \times r_2 \times r_3}$ is the core coefficients tensor. Choose the truncation error $\varepsilon > 0$ for the canonical approximation $\mathbf{P}_R$, then compute the best orthogonal Tucker approximation of $\mathbf{P}$ with tolerance $O(\varepsilon)$ by applying the canonical-to-Tucker algorithm [31] to the canonical tensor $\mathbf{P}_R \mapsto \mathbf{T}_{\mathbf{r}}$. The latter algorithm is based on the rank optimization via ALS iteration. The rank parameters $\mathbf{r}$ of the resultant Tucker approximand $\mathbf{T}_{\mathbf{r}}$ is minimized subject to the ε-error control,

$$\|\mathbf{P}_R - \mathbf{T}_{\mathbf{r}}\| \le \varepsilon \|\mathbf{P}_R\|.$$

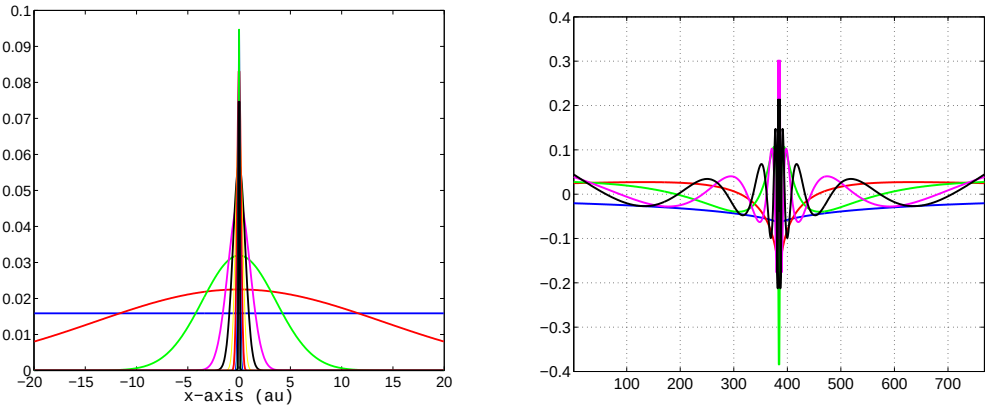

Figure 2.1: Vectors of the canonical $\{\mathbf{p}_q^{(1)}\}_{q=1}^R$ (left) and Tucker $\{\mathbf{t}_k^{(1)}\}_{k=1}^{r_1}$ (right) tensor representations for the single Newton kernel displayed along x-axis.

Remark 2.1 *Since the maximal Tucker rank does not exceed the canonical one we apply the approximation results for canonical tensor to derive the exponential convergence in Tucker rank for the wide class of functions p. This implies the relation* $\max\{r_\ell\} = O(|\log\varepsilon|^2)$ *which can be observed in all numerical test implemented so far.*

Figure 2.1 displays several vectors of the canonical and Tucker tensor representations for a single Newton kernel along x-axis from a set $\{P_q^{(1)}\}_{q=1}^R$. Symmetry of the tensor $\mathbf{P}_R$ implies that the canonical vectors $\mathbf{p}_q^{(2)}$ and $\mathbf{p}_q^{(3)}$ corresponding to y and z-axes, respectively, are of the same shape as $\mathbf{p}_q^{(1)}$. It is clearly seen that there are canonical/Tucker vectors representing the long-, intermediate- and short-range contributions to the total electrostatic potential. This interesting feature will be also recognized for the low-rank lattice sum of potentials (see §3.2).

Table 2.1 presents CPU times (sec) for generating a canonical rank-R tensor approximation of the single Newton kernel over $n \times n \times n$ 3D Cartesian grid, corresponding to Matlab implementation on a terminal of the 8 AMD Opteron Dual-Core processor. The corresponding mesh sizes are given in *A*ngstroms. We observe a logarithmic scaling of the canonical rank R in the grid size n, while the maximal Tucker rank has the tendency to decrease for larger n. The compression rate for the grid 73768^3, that is the ratio $n^3/(nR)$ for the canonical format and $n^3/(3r^3n)$ for the Tucker format are of the order of 10^8 and 10^7, respectively.

grid size n^3	4608^3	9216^3	18432^3	36864^3	73768^3
mesh size h (Å)	0.0019	0.001	$4.9 \cdot 10^{-4}$	$2.8 \cdot 10^{-4}$	$1.2 \cdot 10^{-4}$
Time (Canon.)	2.	2.7	8.1	38	164
Canonical rank R	34	37	39	41	43
Time (C2T)	17	38	85	200	435
Tucker rank	12	11	10	8	6

Table 2.1: CPU times (Matlab) to compute with tolerance $\varepsilon = 10^{-6}$ canonical and Tucker vectors of $\mathbf{P}_R$ for the single Newton kernel in a box.

Notice that the low-rank canonical/Tucker approximation of the tensor $\mathbf{P}$ is the problem independent task, hence the respective canonical/Tucker vectors can be precomputed at once on large enough 3D $n \times n \times n$ grid, and then stored for the multiple use. The storage size is bounded by Rn or $3rn + r^3$.

.

2.2 Low-rank representation for the general class of kernels

Along with Coulombic systems corresponding to $p(\|x\|) = \frac{1}{\|x\|}$, the tensor approximation described above can be also applied to a wide class of commonly used long-range kernels $p(\|x\|)$ in $\mathbb{R}^3$, for example, to the Slater, Yukawa, Lennard-Jones or Van der Waals and dipole-dipole interactions potentials defined as follows.

$$\text{Slater function:} \quad p(\|x\|) = \exp(-\lambda\|x\|), \quad \lambda > 0,$$

$$\text{Yukawa kernel:} \quad p(\|x\|) = \frac{\exp(-\lambda\|x\|)}{\|x\|}, \quad \lambda > 0,$$

$$\text{Lennard-Jones potential:} \quad p(\|x\|) = 4\epsilon \left[\left(\frac{\sigma}{\|x\|} \right)^{12} - \left(\frac{\sigma}{\|x\|} \right)^{6} \right],$$

The simplified version of the Lennard-Jones potential is the so-called Buckingham function

$$\text{Buckingham potential:} \quad p(\|x\|) = 4\epsilon \left[e^{\|x\|/r_0} - \left(\frac{\sigma}{\|x\|} \right)^{6} \right].$$

The electrostatic potential energy for the dipole-dipole interaction due to Van der Waals forces is defined by

$$\text{Dipole-dipole interaction energy:} \quad p(\|x\|) = \frac{C_0}{\|x\|^3}.$$

The quasi-optimal low-rank decompositions based on the *sinc*-quadrature approximation to the Laplace transforms of the above mentioned functions can be rigorously proven foe a wide class of generating kernels. In particular, the following Laplace (or Laplace-Gauss) integral transforms [45] with a parameter $\rho > 0$ can be applied for the sinc-quadrature approximation of the above mentioned functions,

$$e^{-2\sqrt{\kappa\rho}} = \frac{\sqrt{\kappa}}{\sqrt{\pi}} \int_{\mathbb{R}_+} t^{-3/2} e^{-\kappa/t} \, e^{-\rho t} dt, \tag{2.7}$$

$$\frac{e^{-\kappa\sqrt{\rho}}}{\sqrt{\rho}} = \frac{2}{\sqrt{\pi}} \int_{\mathbb{R}_+} e^{-\kappa^2/t^2} \, e^{-\rho t^2} dt, \tag{2.8}$$

$$\frac{1}{\sqrt{\rho}} = \frac{2}{\sqrt{\pi}} \int_{\mathbb{R}_+} e^{-\rho t^2} dt, \tag{2.9}$$

$$\frac{1}{\rho^n} = \frac{1}{(n-1)!} \int_{\mathbb{R}_+} t^{n-1} e^{-\rho t} dt, \quad n = 1, 2, ... \tag{2.10}$$

combined with the subsequent substitution of a parameter ρ by the appropriate function $\rho(x) = \rho(x_1, x_2, x_3)$ with commonly used additive representation $\rho = x_1^p + x_2^q + x_3^z$. The convergence rate for the *sinc*-quadrature approximations of type (2.3) for the cases (2.10) ($n = 1$) and (2.9) has been considered in [4, 5] and later analyzed in more detail in [16, 19]. The case of the Yukawa and Slater kernel has been investigated in [27, 28]. The exponential error bound for the general transform (2.10) can be derived by minor modifications of the above mentioned results.

For example, in the particular representation (2.8) with $\kappa = 0$, given by (2.9), we set up $\rho = x_1^2 + x_2^2 + x_3^2$, i.e. $p(z) = 1/z$, for $1 \le x_\ell < \infty$ and consider the *sinc*-quadrature approximation as in (2.3),

$$p(z) = \frac{2}{\sqrt{\pi}} \int_{\mathbb{R}_+} e^{-t^2 z^2} \, \mathrm{d}t \approx \sum_{k=-M}^{M} a_k e^{-t_k^2 z^2} \quad \text{for} \quad |z| > 0. \tag{2.11}$$

Now the the lattice sum for some $b > 0$,

$$\Sigma_L(x) = \sum_{i_1,i_2,i_3=1}^{L} \frac{1}{\sqrt{(x_1 + i_1 b)^2 + (x_2 + i_2 b)^2 + (x_3 + i_3 b)^2}},$$

can be represented by the integral transform

$$\begin{aligned} \Sigma_L(x) &= \frac{2}{\sqrt{\pi}} \int_{\mathbb{R}_+} [\sum_{i_1,i_2,i_3=1}^{L} e^{-[(x_1+i_1 b)^2 + (x_2+i_2 b)^2 + (x_3+i_3 b)^2] t^2}] dt \\ &= \frac{2}{\sqrt{\pi}} \int_{\mathbb{R}_+} \sum_{k_1=1}^{L} e^{-(x_1+k_1 b)^2 t} \sum_{k_2=1}^{L} e^{-(x_2+k_2 b)^2 t} \sum_{k_3=1}^{L} e^{-(x_3+k_3 b)^2 t} dt \end{aligned} \tag{2.12}$$

with a separable integrand. Representation (2.12) indicates that applying the same quadrature approximation to the lattice sum integral (2.12) as that for the single kernel (2.11) will lead to the decomposition of the total sum of potentials with the same canonical rank as for the single one.

In the following sections we construct such low-rank canonical and Tucker decompositions of the lattice sum of interaction potentials applied to the general class of kernel functions.

3 Tucker decomposition for lattice sum of potentials

3.1 Direct tensor sum for a moderate number of arbitrarily distributed potentials

Here, we recall the direct tensor summation of the electrostatic potentials for a moderate number of arbitrarily distributed sources introduced in [23, 24]. The basic example in electronic structure calculations is concerned with the nuclear potential operator describing the Coulombic interaction of electrons with the nuclei in a molecular system in a box corresponding to the choice $p(\|x\|) = \frac{1}{\|x\|}$.

We consider a function $v_c(x)$ describing the interaction potential of several nuclei in a box $\Omega = [-b/2, b/2]^3$,

$$v_c(x) = \sum_{\nu=1}^{M_0} Z_\nu p(\|x - a_\nu\|), \quad Z_\nu > 0, \quad x, a_\nu \in \Omega \subset \mathbb{R}^3, \tag{3.1}$$

where M_0 is the number of nuclei in Ω, and a_ν, $Z_\nu > 0$, represent their coordinates and "charges", respectively. We are interested in the low-lank representation of the projected tensor $\mathbf{V}_c$ along the line of §2.1.

Similar to [24, 25], we first approximate the non-shifted kernel $p(\|x\|)$ on the auxiliary extended box $\widetilde{\Omega} = [-b, b]^3$ in the canonical format by its projection onto the basis set $\{\psi_{\mathbf{i}}\}$ of piecewise constant functions as described in Section 2.1, and defined on a $2n \times 2n \times 2n$ uniform tensor grid $\widetilde{\Omega}_{2n}$ with the mesh size h, embedding $\Omega_n \subset \widetilde{\Omega}_{2n}$. This defines the "master" rank-R canonical tensor as above

$$\widetilde{\mathbf{P}}_R = \sum_{q=1}^{R} \widetilde{\mathbf{p}}_q^{(1)} \otimes \widetilde{\mathbf{p}}_q^{(2)} \otimes \widetilde{\mathbf{p}}_q^{(3)} \in \mathbb{R}^{2n \times 2n \times 2n}. \tag{3.2}$$

For ease of exposition, we assume that each nuclei coordinate a_ν is located exactly[1] at a grid-point $a_\nu = (i_\nu h - b/2, j_\nu h - b/2, k_\nu h - b/2)$, with some $1 \le i_\nu, j_\nu, k_\nu \le n$. Now we are able to introduce the rank-1 shift-and-windowing operator

$$\mathcal{W}_\nu = \mathcal{W}_\nu^{(1)} \otimes \mathcal{W}_\nu^{(2)} \otimes \mathcal{W}_\nu^{(3)} : \mathbb{R}^{2n \times 2n \times 2n} \to \mathbb{R}^{n \times n \times n}, \quad \textit{for} \quad \nu = 1, ..., M_0$$

by

$$\mathcal{W}_\nu \widetilde{\mathbf{P}}_R := \widetilde{\mathbf{P}}_R(i_\nu + n/2 : i_\nu + 3/2n; j_\nu + n/2 : j_\nu + 3/2n; k_\nu + n/2 : k_\nu + 3/2n) \in \mathbb{R}^{n \times n \times n}, \tag{3.3}$$

With this notation, the projected tensor $\mathbf{V}_c$ approximating the total electrostatic potentials $v_c(x)$ in Ω is represented by a direct sum of canonical tensors

$$\begin{aligned} \mathbf{V}_c \mapsto \mathbf{P}_c &= \sum_{\nu=1}^{M_0} Z_\nu \mathcal{W}_\nu \widetilde{\mathbf{P}}_R \\ &= \sum_{\nu=1}^{M_0} Z_\nu \sum_{q=1}^{R} \mathcal{W}_\nu^{(1)} \widetilde{\mathbf{p}}_q^{(1)} \otimes \mathcal{W}_\nu^{(2)} \widetilde{\mathbf{p}}_q^{(2)} \otimes \mathcal{W}_\nu^{(3)} \widetilde{\mathbf{p}}_q^{(3)} \in \mathbb{R}^{n \times n \times n}, \end{aligned} \tag{3.4}$$

where every rank-R canonical tensor $\mathcal{W}_\nu \widetilde{\mathbf{P}}_R \in \mathbb{R}^{n \times n \times n}$ is thought as a sub-tensor of the master tensor $\widetilde{\mathbf{P}}_R \in \mathbb{R}^{2n \times 2n \times 2n}$ obtained by its shifting and restriction (windowing) onto the $n \times n \times n$ grid in the box $\Omega_n \subset \widetilde{\Omega}_{2n}$. Here a shift from the origin is specified according to the coordinates of the corresponding nuclei, a_ν, counted in the h-units.

[1] Our approximate numerical scheme is designed for nuclei positioned arbitrarily in the computational box where approximation error of order $O(h)$ is controlled by choosing large enough grid size n. Indeed, $1D$ computational cost enables usage of fine grids of size $n^3 \approx 10^{15}$, yielding mesh size $h \approx 10^{-4} \div 10^{-5}$ $\mathring{A}$, in Matlab implementation (h is of the order of the atomic radii). This grid-based tensor calculation scheme for the nuclear potential operator was tested numerically in molecular calculations [23], where it was compared with the results of analytical evaluation of the same operator from benchmark quantum chemical packages.

For example, the electrostatic potential centered at the origin, i.e. with $a_\nu = 0$, corresponds to the restriction of $\widetilde{\mathbf{P}}_R \in \mathbb{R}^{2n\times 2n\times 2n}$ onto the initial computational box Ω_n, i.e. to the index set (assume that n is even)

$$\{([n/2+i],[n/2+j],[n/2+k])\}, \quad i,j,k \in \{1,...,n\}.$$

The projected tensor $\mathbf{V}_c$ for the function in (3.1) is represented as a canonical tensor $\mathbf{P}_c$ with the trivial bound on its rank $R_c = rank(\mathbf{P}_c) \le M_0 R$, where $R = rank(\mathbf{P}_R)$. However, our numerical tests for moderate size molecules indicate that the tensor ranks of the $(M_0 R)$-term canonical sum representing $\mathbf{P}_{R_c}$ can be considerably reduced, such that $R_c \approx R$. This rank optimization can be implemented, for example, by the multigrid version of the canonical rank reduction algorithm, canonical-Tucker-canonical [31]. The resultant canonical tensor will be denoted by $\mathbf{P}_{R_c}$.

Along the same line, the direct sum in the Tucker format can be represented by using shift-and-windowing projection of the "master" rank-$\mathbf{r}$ Tucker tensor $\widetilde{\mathbf{T}}_{\mathbf{r}} \in \mathbb{R}^{2n\times 2n\times 2n}$,

$$\begin{aligned} \mathbf{V}_c \mapsto \mathbf{T}_c &= \sum_{\nu=1}^{M_0} Z_\nu \mathcal{W}_\nu \widetilde{\mathbf{T}}_{\mathbf{r}} \\ &= \sum_{\nu=1}^{M_0} Z_\nu \sum_{\mathbf{k}=\mathbf{1}}^{\mathbf{r}} b_{\mathbf{k}} \mathcal{W}_\nu^{(1)} \widetilde{\mathbf{t}}_{k_1}^{(1)} \otimes \mathcal{W}_\nu^{(2)} \widetilde{\mathbf{t}}_{k_2}^{(2)} \otimes \mathcal{W}_\nu^{(3)} \widetilde{\mathbf{t}}_{k_3}^{(3)} \in \mathbb{R}^{n\times n\times n}, \end{aligned} \tag{3.5}$$

As in the case of canonical decomposition, the rank reduction procedure based on ALS-type ε-approximation applies to the sum of Tucker tensors, $\mathbf{T}_c$, resulting in the Tucker tensor $\mathbf{T}_{\mathbf{r}_c}$ with the reduced rank $\mathbf{r}_c \approx \mathbf{r}$.

Summary 3.1 *We summarize that a sum of arbitrarily located potentials in a box can be calculated by a shift-and-windowing tensor operation applied to the low-rank canonical/Tucker representations for the "master" tensor. Usually in electronic structure calculations the ε-rank of the resultant tensor sum can be reduced to the quasi-optimal level of the same order as the rank of a single "master" tensor.*

The proposed grid-based representation of a sum of electrostatic potentials $v_c(x)$ in a form of a tensor in the canonical or Tucker formats enables its easy projection to some separable basis set, like GTO-type atomic orbital basis, polynomials or plane waves. The following example illustrates calculation of the Galerkin matrix in tensor format (cf. [23, 24] for the case of electrostatic potential). We show that computing the projection of a sum of potentials onto a given set of basis functions is reduced to a combination of 1D Hadamard and scalar products [31].

Given the set of continuous basis functions, $\{g_\mu(x)\}$, $\mu = 1,...,N_b$, then each of them can be discretized by a third order tensor,

$$\mathbf{G}_\mu = [g_\mu(x_1(i), x_2(j), x_3(k))]_{i,j,k=1}^n \in \mathbb{R}^{n\times n\times n},$$

obtained by sampling of $g_\mu(x)$ at the midpoints $(x_1(i), x_2(j), x_3(k))$ of the grid-cells indexed by (i,j,k). Suppose, for simplicity, that it is a rank-1 canonical tensor, $rank(\mathbf{G}_\mu) = 1$, i.e.

$$\mathbf{G}_\mu = \mathbf{g}_\mu^{(1)} \otimes \mathbf{g}_\mu^{(2)} \otimes \mathbf{g}_\mu^{(3)} \in \mathbb{R}^{n\times n\times n},$$

with the canonical vectors $\mathbf{g}_\mu^{(\ell)} \in \mathbb{R}^n$, associated with mode $\ell = 1, 2, 3$.

Suppose that a sum of potentials in a box, $v_c(x)$, given by (3.1), is considered as a multiplicative potential in certain operator (say, the Hartree-Fock/Kohn-Sham Hamiltonian). Following [23, 24], we describe its representation in the given basis set by the Galerkin matrix, $V_c = \{v_{km}\} \in \mathbb{R}^{N_b \times N_b}$, whose entries are calculated (approximated) by the simple tensor operations,

$$v_{km} = \int_{\mathbb{R}^3} v_c(x) g_k(x) g_m(x) dx \approx \langle \mathbf{G}_k \odot \mathbf{G}_m, \mathbf{P}_{R_c} \rangle, \quad 1 \le k, m \le N_b. \tag{3.6}$$

Here $\mathbf{P}_{R_c}$ is a sum of shifted/windowed canonical tensors $\mathbf{P}_c$ representing the total electrostatic potential of atoms in a molecule, and

$$\mathbf{G}_k \odot \mathbf{G}_m := (\mathbf{g}_k^{(1)} \odot \mathbf{g}_m^{(1)}) \otimes (\mathbf{g}_k^{(2)} \odot \mathbf{g}_m^{(2)}) \otimes (\mathbf{g}_k^{(3)} \odot \mathbf{g}_m^{(3)})$$

denotes the Hadamard (entrywise) product of rank-1 tensors, represented in terms of 1D Hadamard products. The similar calculations are performed by substitution of tensor $\mathbf{P}_{R_c}$ to the Tucker approximation $\mathbf{T}_{\mathbf{r}_c}$.

The scalar product $\langle \cdot, \cdot \rangle$ in (3.6) is also reduced to 1D scalar products in case of both canonical and Tucker tensors.

Similar to the case of Galerkin projection, many other tensor operations on the canonical/Tucker representations of $\mathbf{V}_c$ can be calculated with the linear cost $O(n)$.

To conclude this section, we notice that the approximation error $\varepsilon > 0$ caused by a separable representation of the nuclear potential is controlled by the rank parameter $R_c = rank(\mathbf{P}_{R_c}) \approx C\,R$, where C mildly depends on the number of nuclei M_0 in a sum (as mentioned above). Now letting $rank(\mathbf{G}_m) = 1$ implies that each matrix element is to be computed with linear complexity in n, $O(R\,n)$. The exponential convergence of the canonical approximation in the rank parameter R allows us the optimal choice $R = O(|\log \varepsilon|)$ adjusting the overall complexity bound $O(|\log \varepsilon|\, n)$, independent on M_0. Similar argument applies to the Tucker approximation.

3.2 Assembled lattice sums in a box by using the Tucker format

In this section, we introduce the efficient scheme for fast agglomerated tensor summation on a lattice in a box in the Tucker format applied to the general interaction potentials.

Given the potential sum v_c in the unit reference cell $\Omega = [-b/2, b/2]^d$, $d = 3$, of size $b \times b \times b$, we consider an interaction potential in a bounded box

$$\Omega_L = B_1 \times B_2 \times B_3,$$

consisting of a union of $L_1 \times L_2 \times L_3$ unit cells $\Omega_{\mathbf{k}}$, obtained by a shift of Ω that is a multiple of b in each variable, and specified by the lattice vector $b\mathbf{k}$, $\mathbf{k} = (k_1, k_2, k_3) \in \mathbb{Z}^d$, $0 \le k_\ell \le L_\ell - 1$ for $L_\ell \in \mathbb{N}$, $(\ell = 1, 2, 3)$. Here $B_\ell = [-b/2, b/2 + (L_\ell - 1)b]$, such that the case $L_\ell = 1$ corresponds to one-layer systems in the variable x_ℓ. Recall that by the construction $b = nh$, where $h > 0$ is the mesh-size (same for all spacial variables).

In the case of an lattice-type atomic/molecular system in a box the summation problem for the total potential $v_{c_L}(x)$ is formulated in the rectangular volume $\Omega_L = \bigcup_{k_1,k_2,k_3=0}^{L-1} \Omega_{\mathbf{k}}$,

where for ease of exposition we consider a lattice of equal sizes $L_1 = L_2 = L_3 = L$. Figure 3.1 illustrates an example of a 3D lattice structure in a box. In general, the volume box for calculations is larger than Ω_L, say with a factor of 2.

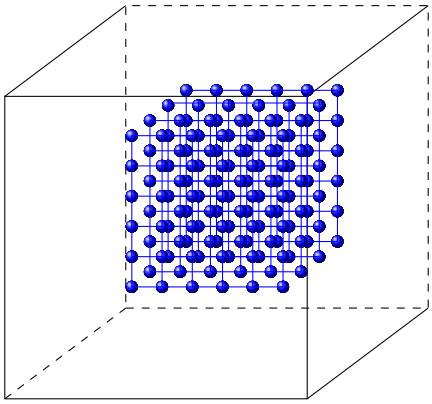

Figure 3.1: Rectangular $6 \times 6 \times 4$ lattice in a box.

Now the potential $v_{c_L}(x)$, for $x \in \Omega_L$ is obtained by summation over all unit cells $\Omega_{\mathbf{k}}$ in Ω_L,

$$v_{c_L}(x) = \sum_{\nu=1}^{M_0} Z_\nu \sum_{k_1,k_2,k_3=0}^{L-1} p(\|x - a_\nu - b\mathbf{k}\|), \quad x \in \Omega_L. \tag{3.7}$$

Note that conventionally this calculation is performed at each of L^3 unit cells $\Omega_{\mathbf{k}} \subset \Omega_L$, which presupposes substantial numerical costs at least of the order of $O(L^3)$. The approach presented in this paper applies to $L \times L \times L$ lattices allows to essentially reduce these costs to linear scaling in L.

Let Ω_{N_L} be the $N_L \times N_L \times N_L$ uniform grid on Ω_L with the same mesh-size h as above, and introduce the corresponding space of piecewise constant basis functions of the dimension N_L^3. In this construction we have $N_L = Ln$. In the case of canonical sums we follow [25], and employ, similar to (3.2), the rank-R "master" tensor defined on the auxiliary box $\widetilde{\Omega}_L$ by scaling Ω_L with a factor of 2,

$$\widetilde{\mathbf{P}}_{L,R} = \sum_{q=1}^{R} \widetilde{\mathbf{p}}_q^{(1)} \otimes \widetilde{\mathbf{p}}_q^{(2)} \otimes \widetilde{\mathbf{p}}_q^{(3)} \in \mathbb{R}^{2N_L \times 2N_L \times 2N_L}. \tag{3.8}$$

Along the same line, we introduce the rank-$\mathbf{r}$ "master" Tucker tensor $\widetilde{\mathbf{T}}_{L,\mathbf{r}} \in \mathbb{R}^{2N_L \times 2N_L \times 2N_L}$.

The next theorem generalizes Theorem 3.1 in [25] to the case of general function $p(\|x\|)$ in (3.7) as well as to the case of Tucker tensor decompositions. It proves the storage and numerical costs for the lattice sum of single potentials (corresponding to the choice $M_0 = 1$, and $a_1 = 0$ in (3.7)), each represented by a rank-R canonical or rank-$\mathbf{r}$ Tucker tensors. In this case the windowing operator $\mathcal{W} = \mathcal{W}_{(\mathbf{k})} = \mathcal{W}_{(k_1)} \otimes \mathcal{W}_{(k_2)} \otimes \mathcal{W}_{(k_3)}$ specifies a shift by the lattice vector $b\mathbf{k}$.

Theorem 3.2 *(A) Given the rank-R canonical "master" tensor, (3.8), approximating the potential $p(\|x\|)$. The projected tensor of the interaction potential, $\mathbf{V}_{c_L}$, representing the full*

lattice sum over L^3 charges can be presented by the rank-R canonical tensor $\mathbf{P}_{c_L}$,

$$\mathbf{P}_{c_L} = \sum_{q=1}^{R} (\sum_{k_1=0}^{L-1} \mathcal{W}_{(k_1)} \widetilde{\mathbf{p}}_q^{(1)}) \otimes (\sum_{k_2=0}^{L-1} \mathcal{W}_{(k_2)} \widetilde{\mathbf{p}}_q^{(2)}) \otimes (\sum_{k_3=0}^{L-1} \mathcal{W}_{(k_3)} \widetilde{\mathbf{p}}_q^{(3)}). \tag{3.9}$$

The numerical cost and storage size are estimated by $O(RLN_L)$ and $O(RN_L)$, respectively, where $N_L = nL$ is the univariate grid size.

(B) Given the rank-$\mathbf{r}$ "master" Tucker tensor $\widetilde{\mathbf{T}}_{L,\mathbf{r}} \in \mathbb{R}^{2N_L \times 2N_L \times 2N_L}$, approximating the potential $p(\|x\|)$. The rank-$\mathbf{r}$ Tucker approximation of a lattice-sum tensor $\mathbf{V}_{c_L}$ can be computed in the form

$$\mathbf{T}_{c_L} = \sum_{\mathbf{m}=\mathbf{1}}^{\mathbf{r}} b_{\mathbf{m}} (\sum_{k_1=0}^{L-1} \mathcal{W}_{(k_1)} \widetilde{\mathbf{t}}_{m_1}^{(1)}) \otimes (\sum_{k_2=0}^{L-1} \mathcal{W}_{(k_2)} \widetilde{\mathbf{t}}_{m_2}^{(2)}) \otimes (\sum_{k_3=0}^{L-1} \mathcal{W}_{(k_3)} \widetilde{\mathbf{t}}_{m_3}^{(3)}). \tag{3.10}$$

The numerical cost and storage size are estimated by $O(3rLN_L)$ and $O(3rN_L)$, respectively.

Proof. For the moment, we fix index $\nu = 1$ in (3.7), set $a_\nu = 0$, and consider only the second sum defined on the complete domain Ω_L,

$$v_{c_L}(x) = Z_1 \sum_{k_1,k_2,k_3=0}^{L-1} p(\|x - b\mathbf{k}\|), \quad x \in \Omega_L. \tag{3.11}$$

Then the projected tensor representation of $v_{c_L}(x)$ takes the form (omitting factor Z)

$$\mathbf{P}_{c_L} = \sum_{k_1,k_2,k_3=0}^{L-1} \mathcal{W}_{\nu(\mathbf{k})} \widetilde{\mathbf{P}}_{L,R} = \sum_{k_1,k_2,k_3=0}^{L-1} \sum_{q=1}^{R} \mathcal{W}_{(\mathbf{k})} (\widetilde{\mathbf{p}}_q^{(1)} \otimes \widetilde{\mathbf{p}}_q^{(2)} \otimes \widetilde{\mathbf{p}}_q^{(3)}) \in \mathbb{R}^{N_L \times N_L \times N_L},$$

where the 3D shift vector is defined by $\mathbf{k} \in \mathbb{Z}^{L \times L \times L}$. Taking into account the separable representation of the Ω_L-windowing operator (tracing onto $N_L \times N_L \times N_L$ window),

$$\mathcal{W}_{(\mathbf{k})} = \mathcal{W}_{(k_1)}^{(1)} \otimes \mathcal{W}_{(k_2)}^{(2)} \otimes \mathcal{W}_{(k_3)}^{(3)},$$

we reduce the above summation to

$$\mathbf{P}_{c_L} = \sum_{q=1}^{R} \sum_{k_1,k_2,k_3=0}^{L-1} \mathcal{W}_{(k_1)} \widetilde{\mathbf{p}}_q^{(1)} \otimes \mathcal{W}_{(k_2)} \widetilde{\mathbf{p}}_q^{(2)} \otimes \mathcal{W}_{(k_3)} \widetilde{\mathbf{p}}_q^{(3)}. \tag{3.12}$$

To reduce the large sum over the full 3D lattice, we use the following property of a sum of canonical tensors with equal ranks R, $\mathbf{C} = \mathbf{A} + \mathbf{B}$, and with two coinciding factor matrices, say for $\ell = 1, 2$: the concatenation in the remaining mode $\ell = 3$ can be reduced to a pointwise summation of the respective canonical vectors,

$$C^{(3)} = [\mathbf{a}_1^{(3)} + \mathbf{b}_1^{(3)}, \ldots, \mathbf{a}_R^{(3)} + \mathbf{b}_R^{(3)}], \tag{3.13}$$

while the first two mode vectors remain unchanged, $C^{(1)} = A^{(1)}$, $C^{(2)} = A^{(2)}$. This preserves the same rank parameter R for the resulting sum. Notice that for each fixed q the inner sum

in (3.12) satisfies the above property. Repeatedly applying this property to a large number of canonical tensors, the 3D-sum (3.12) can be simplified to a rank-R tensor obtained by 1D summations only,

$$\begin{aligned}\mathbf{P}_{c_L} &= \sum_{q=1}^{R}(\sum_{k_1=0}^{L-1}\mathcal{W}_{(k_1)}\widetilde{\mathbf{p}}_q^{(1)}) \otimes (\sum_{k_2,k_3=0}^{L-1}\mathcal{W}_{(k_2)}\widetilde{\mathbf{p}}_q^{(2)} \otimes \mathcal{W}_{(k_3)}\widetilde{\mathbf{p}}_q^{(3)}) \\ &= \sum_{q=1}^{R}(\sum_{k_1=0}^{L-1}\mathcal{W}_{(k_1)}\widetilde{\mathbf{p}}_q^{(1)}) \otimes (\sum_{k_2=0}^{L-1}\mathcal{W}_{(k_2)}\widetilde{\mathbf{p}}_q^{(2)}) \otimes (\sum_{k_3=0}^{L-1}\mathcal{W}_{(k_3)}\widetilde{\mathbf{p}}_q^{(3)}).\end{aligned}$$

The numerical cost are estimated using the standard properties of canonical tensors.

We apply the similar argument in the case of Tucker representation to obtain

$$\begin{aligned}\mathbf{T}_{c_L} &= \sum_{k_1,k_2,k_3=0}^{L-1}\mathcal{W}_{(\mathbf{k})}\widetilde{\mathbf{T}}_{L,\mathbf{r}} \\ &= \sum_{\mathbf{m}=\mathbf{1}}^{\mathbf{r}} b_{\mathbf{m}}(\sum_{k_1=0}^{L-1}\mathcal{W}_{(k_1)}\widetilde{\mathbf{t}}_{m_1}^{(1)}) \otimes (\sum_{k_2=0}^{L-1}\mathcal{W}_{(k_2)}\widetilde{\mathbf{t}}_{m_2}^{(2)}) \otimes (\sum_{k_3=0}^{L-1}\mathcal{W}_{(k_3)}\widetilde{\mathbf{t}}_{m_3}^{(3)}).\end{aligned}$$

This completes the proof. ■

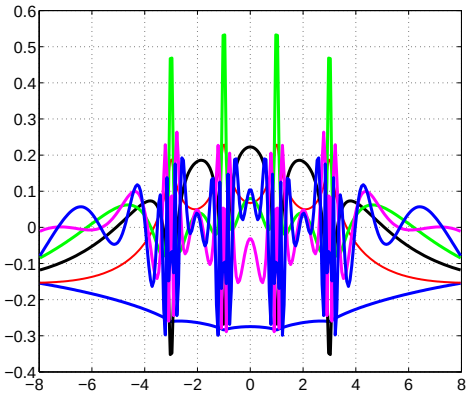

Figure 3.2: Assembled Tucker vectors by using $\widetilde{\mathbf{t}}_{m_1}^{(1)}$ along the x-axis, for a sum over lattice $4 \times 4 \times 1$.

Remark 3.3 *For the general case $M_0 > 1$, the weighted summation over M_0 charges leads to the canonical tensor representation on the "master" unit cell, which can be applied to obtain the rank-R_c representation on the whole $L \times L \times L$ lattice*

$$\mathbf{P}_{c_L} = \sum_{q=1}^{R_c}(\sum_{k_1=0}^{L-1}\mathcal{W}_{(k_1)}\widetilde{\mathbf{p}}_q^{(1)}) \otimes (\sum_{k_2=0}^{L-1}\mathcal{W}_{(k_2)}\widetilde{\mathbf{p}}_q^{(2)}) \otimes (\sum_{k_3=0}^{L-1}\mathcal{W}_{(k_3)}\widetilde{\mathbf{p}}_q^{(3)}). \tag{3.14}$$

Likewise, the rank-$\mathbf{r}_c$ Tucker approximation of a tensor $\mathbf{V}_{c_L}$ can be computed in the form

$$\mathbf{T}_{c_L} = \sum_{\mathbf{m}=\mathbf{1}}^{\mathbf{r}_c} b_{\mathbf{m}}(\sum_{k_1=0}^{L-1}\mathcal{W}_{(k_1)}\widetilde{\mathbf{t}}_{m_1}^{(1)}) \otimes (\sum_{k_2=0}^{L-1}\mathcal{W}_{(k_2)}\widetilde{\mathbf{t}}_{m_2}^{(2)}) \otimes (\sum_{k_3=0}^{L-1}\mathcal{W}_{(k_3)}\widetilde{\mathbf{t}}_{m_3}^{(3)}). \tag{3.15}$$

The next remark generalizes the basic construction to the case of non-uniformly spaced positions of the lattice points.

Remark 3.4 *The previous construction was described for the uniformly spaced positions of charges. However, the agglomerated tensor summation method in both canonical and Tucker formats applies without modifications to a non-equidistant $L_1 \times L_2 \times L_3$ tensor lattice. This is not possible for traditional Ewald summation methods based on FFT transform.*

Figure 3.2 illustrates the shape of several Tucker vectors obtained from $\{\widetilde{\mathbf{t}}^{(1)}_{m_1}\}$ along x-axis. Note that the assembled Tucker vectors do not preserve the initial orthogonality of $\{\widetilde{\mathbf{t}}^{(1)}_{m_1}\}$. It is seen that assembled Tucker vectors accumulate simultaneously the contributions of all single potentials involved in the total sum.

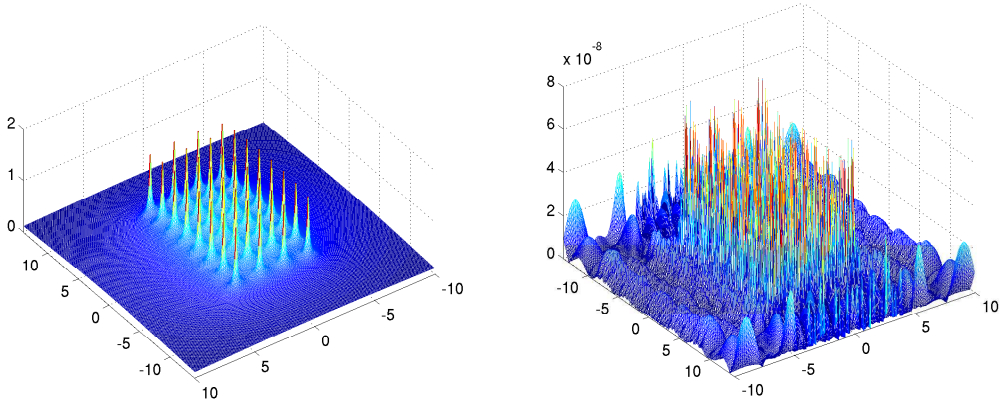

Figure 3.3: Left: Sum of Newton potentials on a $8 \times 4 \times 1$ lattice generated in a volume with the 3D grid size $14336 \times 10240 \times 7168$. Right: the absolute error for the Tucker approximation $(8 \cdot 10^{-8})$.

L^3	4096	32768	262144	2097152
Time	1.8	0.8	3.1	15.8
N_L^3	5632^3	9728^3	17920^3	34304^3

Table 3.1: Time in seconds vs. the total number of potentials L^3 in the the assembled Tucker calculation of the lattice potential sum $\mathbf{P}_{c_L}$. Mesh size (for all grids) is $h = 0.0034$ $\mathring{A}$.

Both the Tucker and canonical tensor representations (3.9) reduce dramatically the numerical costs and storage consumptions. Table 3.1 illustrates complexity scaling $O(N_L L)$ for tensor lattice summation in a box of size $L \times L \times L$ and with the grid-size $N_L \times N_L \times N_L$, where $N_L = n\,L$. This complexity scaling confirms our theoretical estimates.

Figure 3.3 shows the sum of Newton kernels on a lattice $8 \times 4 \times 1$ and the respective Tucker summation error achieved for the Tucker rank $\mathbf{r} = (16, 16, 16)$ representation on the large 3D grid. The spacial mesh size is about 0.002 atomic units (0.001 Å).

Figure 3.4 represents the Tucker vectors obtained from the canonical-to-Tucker decomposition of the assembled canonical tensor sum of potentials on a $8 \times 4 \times 1$ lattice. In this case the Tucker vectors are orthogonal.

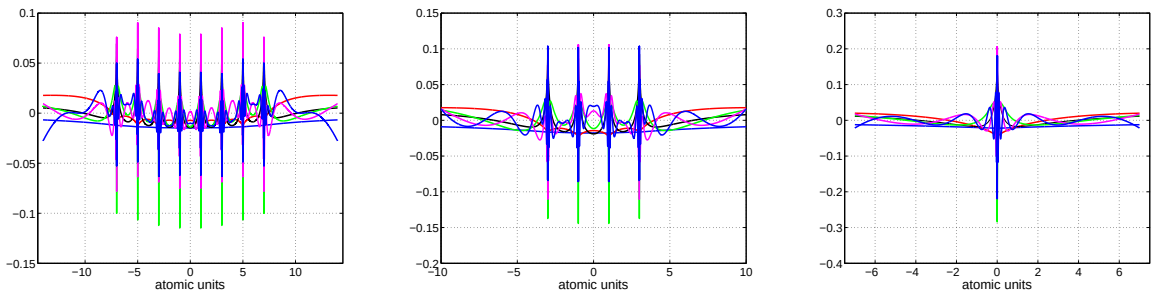

Figure 3.4: Several mode vectors from the C2T representation visualized along x, y- and z-axis on a $8 \times 4 \times 1$ lattice.

4 Tucker representation for lattice sums with defects

4.1 Problem setting

For the perfect lattice sums the resultant canonical and Tucker tensors are proven to inherit exactly the same rank parameters as those for the single "master" tensor.

In the case of lattice sums with defects, say, vacancies or impurities, counted in the canonical format the canonical rank of the perturbed sum may be reduced by using the RHOSVD algorithm, Can $\mapsto$ Tuck $\mapsto$ Can, proposed in [31]. This approach basically provides the compressed tensor with the canonical rank quadratically proportional to those of the respective Tucker approximation to the sum with defects.

In the case of lattice sum in the Tucker format we propose the generalization to the RHOSVD algorithm, now applicable directly to a large sum of Tucker tensors. In this way the initial RHOSVD algorithm in [31] can be viewed as the special case of generalized RHOSVD algorithm applied to a sum of rank-one Tucker tensors. The stability of the new rank reduction method can be proven under mild assumptions on the "weak orthogonality" of the Tucker tensors representing defects in the lattice sum. The numerical complexity of the generalized RHOSVD algorithm scales only linearly in the number of vacancies.

In the following we analyze the assembled Tucker summation of the lattice potentials in the presence of vacancies and impurities. Let us introduce a set of $\mathbf{k}$ lattice indices, $\mathcal{S} =: \{\mathbf{k}_1, ..., \mathbf{k}_S\}$, where the respective Tucker tensor $\mathbf{T}_\mathbf{k}$ for $\mathbf{k} \in \mathcal{S}$ initially given by (3.10) is perturbed by the defect Tucker tensor $\mathbf{U}_\mathbf{k} = \mathbf{U}_s$ $(s = 1, ..., S)$ given by,

$$\mathbf{U}_s = \sum_{\mathbf{m}=\mathbf{1}}^{\mathbf{r}_s} b_{s,\mathbf{m}} \mathbf{u}^{(1)}_{s,m_1} \otimes \mathbf{u}^{(2)}_{s,m_2} \otimes \mathbf{u}^{(3)}_{s,m_3}, \quad s = 1, ..., S. \tag{4.1}$$

Then the non-perturbed Tucker tensor $\mathbf{T}_{c_L}$, further denoted by $\mathbf{U}_0$ (for ease of exposition),

will be substituted by a sum of Tucker tensors,

$$\mathbf{T}_{c_L} \mapsto \widehat{\mathbf{U}} = \mathbf{U}_0 + \sum_{s=1}^{S} \mathbf{U}_s \tag{4.2}$$

with the upper rank estimates for best Tucker approximation of $\widehat{\mathbf{U}}$,

$$\widehat{r}_\ell \le r_{0,\ell} + \sum_{s=1,...,S} r_{s,\ell}, \quad \text{for} \quad \ell = 1, 2, 3.$$

Without loss of generality, all Tucker tensors $\mathbf{U}_s$, $(s = 0, 1, ..., S)$, can be assumed orthogonal. If the number of perturbed cells, S, is large enough, the numerical computations with the Tucker tensor of rank $\widehat{r}_\ell$ becomes prohibitive.

4.2 Lattice sum of canonical tensors with defects: Use of the canonical-to-Tucker approximation

We first consider a sum of canonical tensors with defects. For the readers convenience, we recall the error estimate for RHOSVD approximation to sums of canonical tensors [31]. This applies to arbitrary dimension d, though in our particular application we have $d = 3$. Given a rank parameter $R \in \mathbb{N}$, we denote by

$$\mathbf{A}_{(R)} = \sum\nolimits_{\nu=1}^{R} \xi_\nu \mathbf{a}_\nu^{(1)} \otimes \ldots \otimes \mathbf{a}_\nu^{(d)}, \quad \xi_\nu \in \mathbb{R}, \tag{4.3}$$

the canonical tensor with normalized vectors $\mathbf{a}_\nu^{(\ell)} \in \mathbb{R}^{n_\ell}$ $(\ell = 1, ..., d)$ that is a sum rank-1 canonical/Tucker tensors. The minimal parameter R in (4.3) is called the rank (or canonical rank) of a tensor. For the ease of constructions it is useful to represent this tensor in the Tucker format. Indeed, introducing the side-matrices by concatenation of the corresponding canonical vectors in (4.3),

$$A^{(\ell)} = \left[\mathbf{a}_1^{(\ell)} ... \mathbf{a}_R^{(\ell)}\right], \quad A^{(\ell)} \in \mathbb{R}^{n \times R},$$

and the diagonal tensor (the Tucker core tensor) $\boldsymbol{\xi} := \mathrm{diag}\{\xi_1, ..., \xi_R\} \in \mathbb{R}^{R \times R \times R}$ such that $\xi_{\nu_1,...,\nu_d} = 0$ except when $\nu_1 = ... = \nu_d$ with $\xi_{\nu,...,\nu} = \xi_\nu$ $(\nu = 1, ..., R)$, we obtain the equivalent rank-(R, R, R) Tucker representation

$$\mathbf{A}_{(R)} = \boldsymbol{\xi} \times_1 A^{(1)} \times_2 A^{(2)} ... \times_d A^{(d)}. \tag{4.4}$$

For the readers convenience, we recall (see [31]) the *errorestimates* for the reduced rank-$\mathbf{r}$ HOSVD type Tucker approximation to the tensor in (4.3). We set $n_\ell = n$ and suppose for definiteness that $n \le R$, so that SVD of the side-matrix $A^{(\ell)}$ is given by

$$A^{(\ell)} = Z^{(\ell)} D_\ell V^{(\ell)T} = \sum_{k=1}^{n} \sigma_{\ell,k} \mathbf{z}_k^{(\ell)} \, \mathbf{v}_k^{(\ell)T}, \quad \mathbf{z}_k^{(\ell)} \in \mathbb{R}^n, \ \mathbf{v}_k^{(\ell)} \in \mathbb{R}^R,$$

with the orthogonal matrices $Z^{(\ell)} = [\mathbf{z}_1^{(\ell)}, ..., \mathbf{z}_n^{(\ell)}]$, and $V^{(\ell)} = [\mathbf{v}_1^{(\ell)}, ..., \mathbf{v}_n^{(\ell)}]$, $\ell = 1, ..., d$. Given rank parameters $r_1, ..., r_\ell < n$, introduce the truncated SVD of the side-matrix $A^{(\ell)}$, $Z_0^{(\ell)} D_{\ell,0} V_0^{(\ell)T}$, $(\ell = 1, ..., d)$, where $D_{\ell,0} = \mathrm{diag}\{\sigma_{\ell,1}, \sigma_{\ell,2}, ..., \sigma_{\ell,r_\ell}\}$ and $Z_0^{(\ell)} \in \mathbb{R}^{n \times r_\ell}$, $V_0^{(\ell)} \in \mathbb{R}^{R \times r_\ell}$, represent the orthogonal factors being the respective sub-matrices in the SVD of $A^{(\ell)}$.

Definition 4.1 *([31]) The reduced HOSVD (RHOSVD) approximation of* $\mathbf{A}$*,* $\mathbf{A}^0_{(\mathbf{r})}$*, is defined as the rank-***r** *Tucker tensor obtained by the projection of* $\mathbf{A}$ *onto the orthogonal matrices of singular vectors* $Z_0^{(\ell)}$*,* $(\ell = 1, ..., d)$*.*

In what follows, we denote by $\mathcal{G}_\ell$ the Grassman manifold that is a factor space with respect to all possible rotations to the Stiefel manifold $\mathcal{M}_\ell$ of orthogonal $n \times r_\ell$ matrices,

$$\mathcal{M}_\ell := \{Y \in \mathbb{R}^{n\times r_\ell} : Y^T Y = I_{r_\ell \times r_\ell}\}, \quad (\ell = 1, ..., d).$$

Theorem 4.2 *(Canonical to Tucker approximation, [31]).*
(a) Let $\mathbf{A} = \mathbf{A}_{(R)}$ *be given by (4.3). Then the minimization problem*

$$\mathbf{A} \in \mathbb{V}_\mathbf{n} : \quad \mathbf{A}_{(\mathbf{r})} = \mathrm{argmin}_{\mathbf{T}\in\mathcal{T}_{\mathbf{r},\mathbf{n}}} \|\mathbf{A} - \mathbf{T}\|_{\mathbb{V}_\mathbf{n}}, \tag{4.5}$$

is equivalent to the dual maximization problem over the Grassman manifolds $\mathcal{G}_\ell$*,*

$$[W^{(1)}, ..., W^{(d)}] = \mathrm{argmax}_{Y^{(\ell)}\in\mathcal{G}_\ell} \left\| \sum_{\nu=1}^{R} \xi_\nu \left({Y^{(1)}}^T \mathbf{a}_\nu^{(1)} \right) \otimes ... \otimes \left({Y^{(d)}}^T \mathbf{a}_\nu^{(d)} \right) \right\|^2_{\mathbb{R}^\mathbf{r}}, \tag{4.6}$$

where $Y^{(\ell)} = [y_1^{(\ell)} ... y_{r_\ell}^{(\ell)}] \in \mathbb{R}^{n\times r_\ell}$ $(\ell = 1, ..., d)$*, and* ${Y^{(\ell)}}^T \mathbf{a}_\nu^{(\ell)} \in \mathbb{R}^{r_\ell}$*.*

(b) The compatibility condition $r_\ell \le rank(A^{(\ell)})$ *with* $A^{(\ell)} = [\mathbf{a}_1^{(\ell)} ... \mathbf{a}_R^{(\ell)}] \in \mathbb{R}^{n\times R}$*, ensures the solvability of (4.6). The maximizer is given by orthogonal matrices* $W^{(\ell)} = [\mathbf{w}_1^{(\ell)} ... \mathbf{w}_{r_\ell}^{(\ell)}] \in \mathbb{R}^{n\times r_\ell}$*, which can be computed by ALS Algorithm with the initial guess chosen as the reduced HOSVD approximation of* $\mathbf{A}$*,* $\mathbf{A}^0_{(\mathbf{r})}$*, see Definition 4.1.*

(c) The minimizer in (4.5) is then calculated by the orthogonal projection

$$\mathbf{A}_{(\mathbf{r})} = \sum_{\mathbf{k}=\mathbf{1}}^{\mathbf{r}} \mu_\mathbf{k} \mathbf{w}_{k_1}^{(1)} \otimes \cdots \otimes \mathbf{w}_{k_d}^{(d)}, \quad \mu_\mathbf{k} = \langle \mathbf{w}_{k_1}^{(1)} \otimes \cdots \otimes \mathbf{w}_{k_d}^{(d)}, \mathbf{A} \rangle,$$

where the core tensor $\boldsymbol{\mu} = [\mu_\mathbf{k}]$ *can be represented in the rank-*R *canonical format*

$$\boldsymbol{\mu} = \sum_{\nu=1}^{R} \xi_\nu ({W^{(1)}}^T \mathbf{u}_\nu^{(1)}) \otimes \cdots \otimes ({W^{(d)}}^T \mathbf{u}_\nu^{(d)}).$$

(d) Let $\sigma_{\ell,1} \ge \sigma_{\ell,2} ... \ge \sigma_{\ell,\min(n,R)}$ *be the singular values of the* ℓ*-mode side-matrix* $U^{(\ell)} \in \mathbb{R}^{n\times R}$ $(\ell = 1, ..., d)$*. Then the reduced HOSVD approximation* $\mathbf{A}^0_{(\mathbf{r})}$ *exhibits the error estimate*

$$\|\mathbf{A} - \mathbf{A}^0_{(\mathbf{r})}\| \le \|\boldsymbol{\xi}\| \sum_{\ell=1}^{d} \Big(\sum_{k=r_\ell+1}^{\min(n,R)} \sigma_{\ell,k}^2 \Big)^{1/2}, \quad \textit{where} \quad \|\boldsymbol{\xi}\|^2 = \sum_{\nu=1}^{R} \xi_\nu^2. \tag{4.7}$$

The following assertion proves the stability of RHOSVD approximation.

Lemma 4.3 *The stability condition for decomposition (4.3), i.e.*

$$\sum_{\nu=1}^{R} \xi_\nu^2 \le C \|\mathbf{A}\|^2_{\mathbb{V}_\mathbf{n}}, \tag{4.8}$$

ensures the robust quasi-optimal RHOSVD approximation in the relative norm,

$$\|\mathbf{A} - \mathbf{A}^0_{(\mathbf{r})}\| \le C\|\mathbf{A}\| \sum_{\ell=1}^{d} \Big(\sum_{k=r_\ell+1}^{\min(n,R)} \sigma^2_{\ell,k} \Big)^{1/2}.$$

The stability condition (4.8) is fulfilled, in particular, if (a) all vectors of the canonical decomposition are non-negative that is the case for sinc-quadrature based decompositions to Green's kernels based on integral transforms (2.7) - (2.10); (b) The partial orthogonality of the canonical vectors, i.e. rank-1 tensors $\mathbf{a}^{(1)}_\nu \otimes \ldots \otimes \mathbf{a}^{(d)}_\nu$ *($\nu = 1, ..., R$) are mutually orthogonal.*

4.3 Summation of defects in the Tucker and canonical formats

In the case of Tucker sum (4.2) we define the agglomerated side matrices $\widehat{U}^{(\ell)}$ by concatenation of the directional side-matrices of individual tensors $\mathbf{U}_s$, $s = 0, 1, ..., S$,

$$\widehat{U}^{(\ell)} = [\mathbf{u}^{(\ell)}_1 ... \mathbf{u}^{(\ell)}_{r_{0,\ell}}, \mathbf{u}^{(\ell)}_1 ... \mathbf{u}^{(\ell)}_{r_{1,\ell}}, ..., \mathbf{u}^{(\ell)}_1 ... \mathbf{u}^{(\ell)}_{r_{S,\ell}}] \in \mathbb{R}^{n \times (r_{0,\ell} + \sum_{s=1,...,S} r_{s,\ell})}, \quad \ell = 1, ..., d. \tag{4.9}$$

Given rank parameter $\mathbf{r} = (r_1, ..., r_d)$, introduce the truncated SVD of $\widehat{U}^{(\ell)}$,

$$\widehat{U}^{(\ell)} \approx Z^{(\ell)}_0 D_{\ell,0} {V^{(\ell)}_0}^T, \quad Z^{(\ell)}_0 \in \mathbb{R}^{n \times r_\ell}, \quad {V_0}^{(\ell)} \in \mathbb{R}^{(r_{0,\ell} + \sum_{s=1,...,S} r_{s,\ell}) \times r_\ell},$$

where $D_{\ell,0} = \mathrm{diag}\{\sigma_{\ell,1}, \sigma_{\ell,2}, ..., \sigma_{\ell,r_\ell}\}$.

Items (a) - (d) in Theorem 4.2 can be generalized to the case of Tucker tensors. In particular, the stability criteria for RHOSVD approximation as in Lemma 4.3 allows natural extension to the case of generalized RHOSVD approximation applied to a sum of Tucker tensors in (4.2).

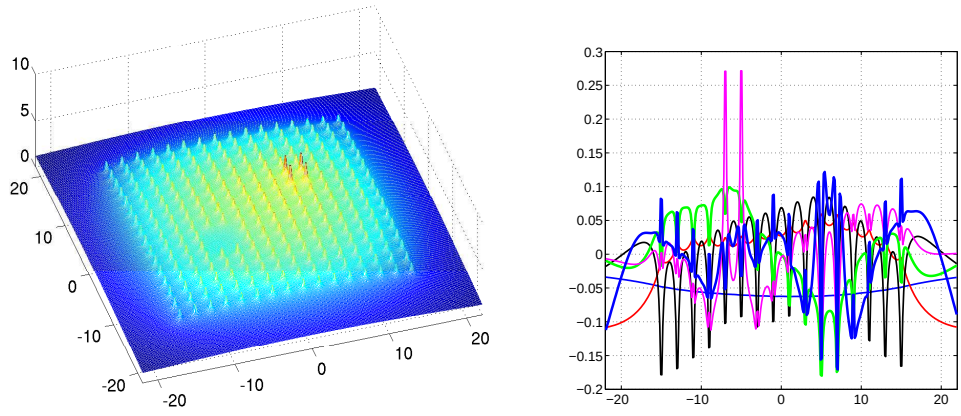

Figure 4.1: Left: assembled Tucker summation of 3D grid-based Newton potentials on a lattice $16 \times 16 \times 1$, with an impurity, of size $2 \times 2 \times 1$. Right: the corresponding Tucker vectors along x-axis.

The following theorem provides the error estimate for the generalized RHOSVD approximation converting a sum of Tucker tensors to a single term with fixed Tucker ranks or subject to given tolerance $\varepsilon > 0$. The resultant Tucker tensor can be considered as the initial guess for the ALS iteration to compute best Tucker ε-approximation of a sum of Tucker tensors.

Theorem 4.4 *(Tucker Sum-to-Tucker)*
Given a sum of Tucker tensors (4.2) and the rank truncation parameter $\mathbf{r} = (r_1, ..., r_d)$.
(a) Let $\sigma_{\ell,1} \geq \sigma_{\ell,2} ... \geq \sigma_{\ell,\min(n,R)}$ *be the singular values of the* ℓ*-mode side-matrix* $\widehat{U}^{(\ell)} \in \mathbb{R}^{n\times R}$ $(\ell = 1, ..., d)$ *defined in (4.9). Then the generalized RHOSVD approximation* $\mathbf{U}^0_{(\mathbf{r})}$ *obtained by the projection of* $\widehat{\mathbf{U}}$ *onto the singular vectors* $Z_0^{(\ell)}$ *of the Tucker side-matrices,* $\widehat{U}^{(\ell)} \approx Z_0^{(\ell)} D_{\ell,0} {V_0^{(\ell)}}^T$, *exhibits the error estimate*

$$\|\widehat{\mathbf{U}} - \mathbf{U}^0_{(\mathbf{r})}\| \leq |\mathbf{B}| \sum_{\ell=1}^{d} \Big(\sum_{k=r_\ell+1}^{\min(n,\widehat{r}_\ell)} \sigma^2_{\ell,k} \Big)^{1/2}, \quad \textit{where} \quad |\mathbf{B}|^2 = \sum_{s=0}^{S} \|\mathbf{B}_s\|^2. \tag{4.10}$$

(b) Assume that the stability condition for the sum (4.2),

$$\sum_{s=0}^{S} \|\mathbf{B}_s\|^2 \leq C \|\widehat{\mathbf{U}}\|^2,$$

is fulfilled, then the generalized RHOSVD approximation provides the quasi-optimal error bound

$$\|\widehat{\mathbf{U}} - \mathbf{U}^0_{(\mathbf{r})}\| \leq \|\widehat{\mathbf{U}}\| \sum_{\ell=1}^{d} \Big(\sum_{k=r_\ell+1}^{\min(n,\widehat{r}_\ell)} \sigma^2_{\ell,k} \Big)^{1/2}.$$

Proof. Proof of item (a) is similar to those for Theorem 4.2, presented in [31]. Item (b) can be justified by straightforward calculation. ∎

Figure 4.1 (left) visualizes result of assembled Tucker summation of 3D grid-based Newton potentials on a $16 \times 16 \times 1$ lattice, with a vacancy and impurity, each of $2 \times 2 \times 1$ lattice size. Figure 4.1 (right) shows the corresponding Tucker vectors along x-axis. These vectors clearly represent the local shape of vacancies and impurities.

Notice that the case of lattice sum of canonical tensors considered in §4.2 can be interpreted as a special case of a sum of Tucker tensors with rank equals to 1, and the number of term $R = S$.

5 Summation over non-rectangular lattices

In some practically interesting cases the physical lattice may have non-rectangular geometry that does not fit exactly the tensor-product structure of the canonical/Tucker data arrays. For example, the hexagonal or parallelepiped type lattices can be considered. The case study of many particular classes of geometries is beyond the scope of our paper. Instead, we formulate the main principles on how to apply tensor summation methods to non-rectangular geometries and give a few examples demonstrating the required (minor) modifications of the basic agglomerated summation schemes described above.

Figure 5.1: Hexagonal lattice is a union of two rectangular lattices, "red" and "blue"

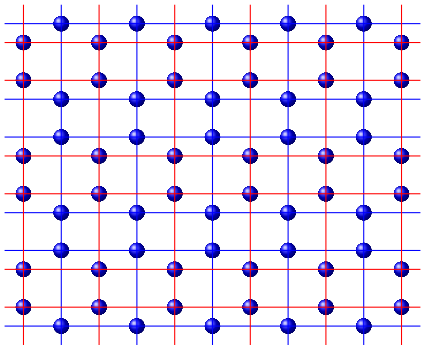

Figure 5.2: Parallelogram-type lattice

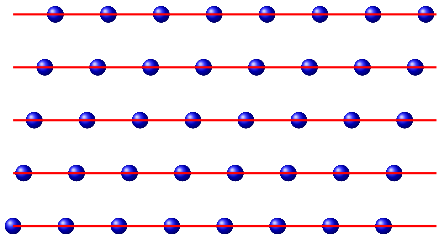

It is worth to note that most of interesting lattice structures (say, arising in crystalline modeling) inherit a number of spacial symmetries which allow, first, to classify and then simplify the computational schemes for each particular case of symmetry. In this concern, we consider the following classes of lattice topologies which can be efficiently treated by our tensor summation techniques:

(A) The target lattice $\mathcal{L}$ can be split into the union of several (few) sub-lattices, $\mathcal{L} = \bigcup \mathcal{L}_q$, such that each sub-lattice $\mathcal{L}_q$ allows a 3D rectangular grid-structure.

(B) The 3D lattice points belong to the rectangular tensor grid in two spatial coordinates, but they violate the tensor structure in the third variable (say, parallelogram type grids).

(C) The 3D lattice points belong to the tensor grid in one of spatial coordinate, but they may violate the rectangular tensor structure in the remaining couple of variables.

(D) Defects in the target lattice are distributed over rectangular sub-lattices on several coarser scales (multi-level tensor lattice sum).

In case (A) the agglomerated tensor summation algorithms apply independently to each rectangular sub-lattice $\mathcal{L}_q$, and then the target tensor is obtained as a direct sum of tensors associated with $\mathcal{L}_q$, supplemented by the subsequent rank reduction procedure. The example of such a geometry is given by hexagonal grid presented in Figure 5.1 ((x, y) section of the 3D lattice, that is rectangular in z-direction), which can be split into a union of two rectangular sub-lattices $\mathcal{L}_1$ (red) and $\mathcal{L}_2$ (blue). Another example is a lattice with step-type boundary. In this case the maximal rank does not exceed the multiple of $\log L$ and the rank of a single reference Tucker tensor.

In case (B) the tensor summation applies only in two indices while a sum in the remaining third index is treated directly. This leads to the increase of directional rank proportionally to the 1D size of the lattice, L, hence requiring the subsequent rank reduction procedures. This may lead to the higher computational complexity of the summation. The example of such a structure is the parallelogram-type lattice shown in Figure 5.2 (orthogonal projection onto (x, y) plane).

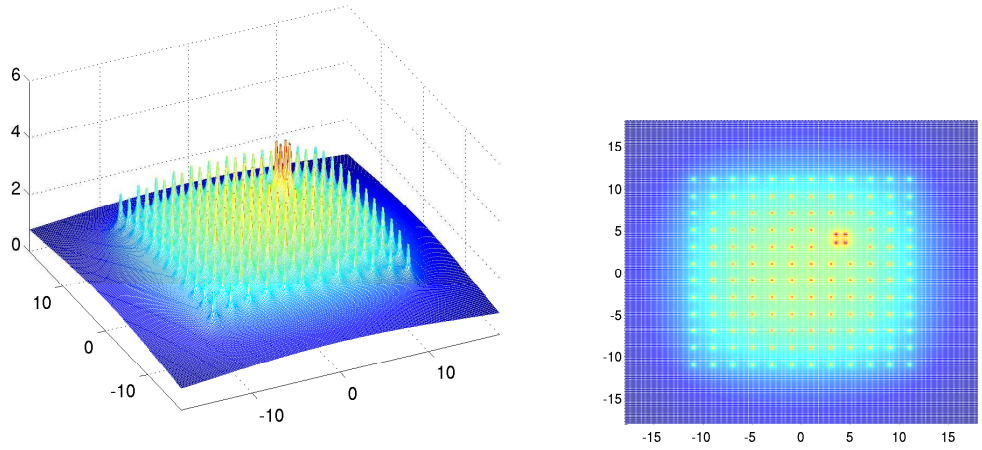

Figure 5.3: Left: assembled canonical summation of 3D grid-based Newton potentials on a lattice $12 \times 12 \times 1$, with an impurity, of size $2 \times 2 \times 1$. Right: the vertical projection.

In case (C) the agglomerated summation can be performed only in one index, supplemented by the direct summation in the remaining indices. The total rank then increases proportionally to L^2, making the subsequent rank optimization procedure indispensible. However, even in this worst case scenario, the asymptotic complexity of the direct summation shall be reduced on the order of magnitude in L from $O(L^3)$, due to the benefits of "one-way" tensor summation.

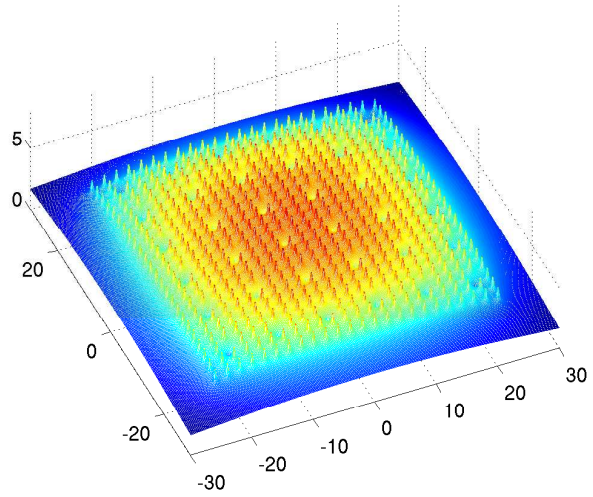

Figure 5.4: Left: assembled canonical summation of 3D grid-based Newton potentials on a lattice $24 \times 24 \times 1$, with regular $6 \times 6 \times 6$ vacancies.

Case (D) can be treated by successive application of the canonical/Tucker tensor summation algorithm at several levels of defects location. Figure 5.3 represent the result of assembled canonical summation of 3D grid-based Newton potentials on a lattice $12 \times 12 \times 1$,

with an impurity of size $2 \times 2 \times 1$ that does not fit the location of lattice points, but determined on the same fine $N_L \times N_L \times N_L$ representation grid. In the case of many non-regularly distributed defects the summation should be implemented in the Tucker format with the subsequent rank truncation. Figure 5.4 visualizes the result of assembled canonical summation of 3D grid-based Newton potentials on a lattice $24 \times 24 \times 1$, with regularly positioned $6 \times 6 \times 6$ vacancies (two-level lattice). Figure 5.5 represents the result of assembled canonical summation of the Newton potentials on L-shaped (left) and O-shaped (right) sub-lattices of the $24 \times 24 \times 1$ lattice (two-level step-type geometry). In all these cases the total tensor rank does not exceed the double rank of the single reference potential since all vacancies are located on tensor sub-lattice of the target lattice.

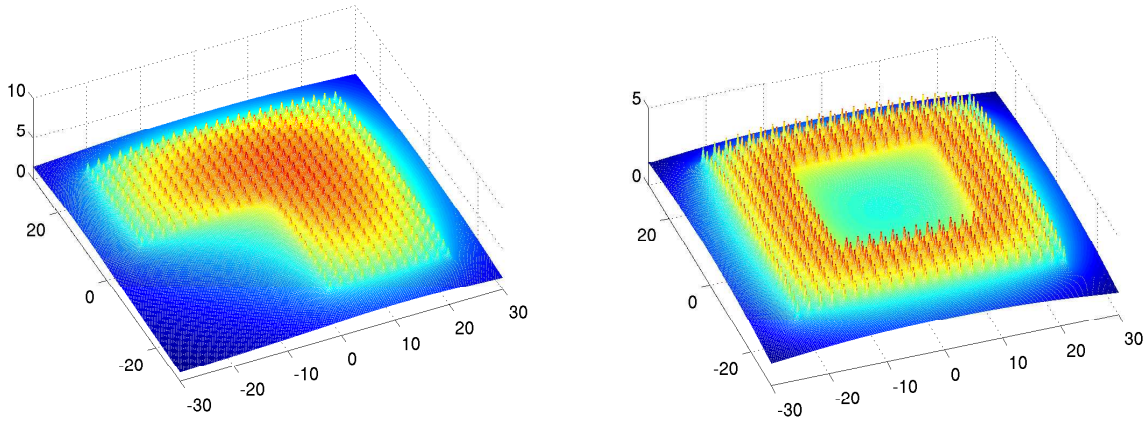

Figure 5.5: Assembled canonical summation of the Newton potentials on L-shaped (left) and O-shaped (right) sub-lattices of the $24 \times 24 \times 1$ lattice.

We summarize that in all cases (A) - (D) classified above the tensor summation approach cab be gainfully applied. The overall numerical cost may depend on the geometric structure and symmetries of the system under consideration since violation of the tensor-product rectangular structure of the lattice may lead to the increase in the Tucker/canonical rank. This is clearly observed in the case of random distribution of the moderate number of defects. In all such cases the RHOSVD approximation combined with the ALS iteration serves for the robust rank reduction in the Tucker format.

6 Conclusions

We introduce the assembled Tucker tensor method for 3D grid-based summation of classical interaction potentials placed onto a large 3D lattice in a box. Examples of such potentials include the Newton, Slater, Yukawa, Lennard-Jones, Buckingham and dipole-dipole kernel functions among others. With slight modifications, the approach also applies in the presence of defects, such as vacancies, impurities or to lattices with non-rectangular set of active points, as well as to the case of non-rectangular lattices.

The computational work for summation over $L \times L \times L$ rectangular or type (A) lattices scales linearly in L, that improves dramatically the cubic costs, $O(L^3)$, of the traditional

Ewald type summation techniques. All data are presented on the common fine 3D $N \times N \times N$ grid by low-rank tensors in $\mathbb{R}^{N\times N\times N}$, that allows the simultaneous approximation with guaranteed precision of all singular kernel functions involved in the summation.

In case of unperturbed lattice, both the canonical and Tucker ranks of the resultant tensor sum remains the same as for the individual potential. In the situation with defects or in the presence of non-rectangular lattice the Tucker ranks of the resultant tensor may increase. Then the ε-rank truncation procedure can be applied to a sum of canonical or Tucker tensors.

Numerical examples illustrate the rank bounds and asymptotic complexity of the tensor summation method in both canonical and Tucker data formats in the agreement with theoretical predictions.

The assembled tensor summation approach is well suited for further application in electronic and molecular structure calculations of large lattice-structured compounds, see [26].

References

[1] C. Bertoglio, and B.N. Khoromskij. *Low-rank quadrature-based tensor approximation of the Galerkin projected Newton/Yukawa kernels.* Comp. Phys. Communications, 183(4) (2012) 904–912.

[2] Bloch, André, "Les theoremes de M. Valiron sur les fonctions entieres et la theorie de l'uniformisation". Annales de la faculte des sciences de l'universite de Toulose 17 (3): 1-22 (1925). ISSN 0240-2963.

[3] Boys, S. F., Cook, G. B., Reeves, C. M. and Shavitt, I. (1956). *Automatic Fundamental Calculations of Molecular Structure.* Nature, 178: 1207-1209.

[4] D. Braess. *Nonlinear approximation theory.* Springer-Verlag, Berlin, 1986.

[5] D. Braess. *Asymptotics for the Approximation of Wave Functions by Exponential-Sums.* J. Approx. Theory, 83: 93-103, (1995).

[6] E. Cancés, V. Ehrlacher, and Y. Maday. *Periodic Schrödinger operator with local defects and spectral pollution.* SIAM J. Numer. Anal. v. 50, No. 6, pp. 3016-3035.

[7] E. Cancés and C. Le Bris. *Mathematical modeling of point defects in materials science.* Math. Methods Models Appl. Sci. 23 (2013) 1795-1859.

[8] T. Darten, D. York and L. Pedersen. *Particle mesh Ewald: An $O(N \log N)$ method for Ewald sums in large systems.* J. Chem. Phys., 98, 10089-10091, 1993.

[9] L. De Lathauwer, B. De Moor, J. Vandewalle. *A multilinear singular value decomposition.* SIAM J. Matrix Anal. Appl., 21 (2000) 1253-1278.

[10] M. Deserno and C. Holm. *How to mesh up Ewald sums. I. A theoretical and numerical comparison of various particle mesh routines.* J. Chem. Phys., 109(18): 7678-7693, 1998.

[11] S.V. Dolgov. *Tensor-product methods in numerical simulation of high-dimensional dynamical problems.*, University of Leipzig, Dissertaion, 2014. http://nbn-resolving.de/urn:nbn:de:bsz:15-qucosa-151129

[12] Sergey Dolgov, Boris N. Khoromskij, Alexander Litvinenko, and Hermann G. Matthies. *Computation of the Response Surface in the Tensor Train data format.* E-preprint arXiv:1406.2816, 2014.

[13] R. Dovesi, R. Orlando, C. Roetti, C. Pisani, and V.R. Sauders. *The Periodic Hartree-Fock Method and its Implementation in the CRYSTAL Code.* Phys. Stat. Sol. (b) **217**, 63 (2000).

[14] V. Ehrlacher, C. Ortner, and A. V. Shapeev. *Analysis of boundary conditions for crystal defect atomistic simulations.* e-prints ArXiv:1306.5334, 2013.

[15] Ewald P.P. *Die Berechnung optische und elektrostatischer Gitterpotentiale.* Ann. Phys **64**, 253 (1921).

[16] I.P. Gavrilyuk, W. Hackbusch and B.N. Khoromskij. *D*ata-Sparse Approximation to a Class of Operator-Valued Functions. Math. Comp. **74** (2005), 681-708.

[17] L. Grasedyck, D. Kressner and C. Tobler. *A literature survey of low-rank tensor approximation techniques.* arXiv:1302.7121v1, 2013.

[18] L. Greengard and V. Rochlin. *A fast algorithm for particle simulations.* J. Comp. Phys. 73 (1987) 325.

[19] W. Hackbusch and B.N. Khoromskij. *Low-rank Kronecker product approximation to multi-dimensional nonlocal operators. Part I. Separable approximation of multi-variate functions.* Computing **76** (2006), 177-202.

[20] T. Helgaker, P. Jørgensen, and J. Olsen. *Molecular Electronic-Structure Theory.* Wiley, New York, 1999.

[21] Philippe H. Hünenberger. *Lattice-sum methods for computing electrostatic interactions in molecular simulations.* CP492, L.R. Pratt and G. Hummer, eds., 1999, American Institute of Physics, 1-56396-906-8/99.

[22] Venera Khoromskaia. *Numerical Solution of the Hartree-Fock Equation by Multilevel Tensor-structured methods.* Dissertation, TU Berlin, 2010.
http://opus4.kobv.de/opus4-tuberlin/frontdoor/index/index/docId/2780

[23] V. Khoromskaia, D. Andrae, and B.N. Khoromskij. *Fast and accurate 3D tensor calculation of the Fock operator in a general basis.* Comp. Phys. Communications, 183 (2012) 2392-2404.

[24] V. Khoromskaia. *Black-box Hartree-Fock solver by tensor numerical methods.* Comp. Meth. in Applied Math., Vol. 14 (2014) No.1, pp. 89-111.

[25] V. Khoromskaia and B. N. Khoromskij. *Grid-based lattice summation of electrostatic potentials by assembled rank-structured tensor approximation.* Comp. Phys. Communications, 185 (2014), pp. 3162-3174.

[26] V. Khoromskaia, and B.N. Khoromskij. *Tensor Approach to Linearized Hartree-Fock Equation for Lattice-type and Periodic Systems.* E-preprint arXiv:1408.3839, 2014 (submitted).

[27] B.N. Khoromskij, *Structured Rank-*$(r_1, ..., r_d)$ *Decomposition of Function-related Tensors in* $\mathbb{R}^d$. Comp. Meth. in Applied Math., **6** (2006), 2, 194-220.

[28] B.N. Khoromskij. *On Tensor Approximation of Green Iterations for Kohn-Sham Equations.* Computing and Visualization in Sci., **11**: 259-271 (2008).

[29] B.N. Khoromskij. $O(d \log N)$*-Quantics Approximation of* N*-*d *Tensors in High-Dimensional Numerical Modeling.* Constructive Approx. **34** (2011) 257–280. (Preprint 55/2009 MPI MiS, Leipzig 2009.)

[30] B. N. Khoromskij and V. Khoromskaia. *Low Rank Tucker Tensor Approximation to the Classical Potentials.* Central European J. of Math., **5**(3) 2007, 1-28.

[31] B.N. Khoromskij and V. Khoromskaia. *Multigrid tensor approximation of function related multi-dimensional arrays.* SIAM J. Sci. Comp. 31(4) (2009) 3002-3026.

[32] B.N. Khoromskij. *Tensors-structured Numerical Methods in Scientific Computing: Survey on Recent Advances.* Chemometr. Intell. Lab. Syst. 110 (2012), 1-19.

[33] Boris N. Khoromskij. *Tensor Numerical Methods for High-dimensional PDEs: Basic Theory and Initial Applications.* E-preprint arXiv:1408.4053, 2014. ESAIM: Proceedings 2014 (to appear).

[34] T.G. Kolda and B.W. Bader. *Tensor Decompositions and Applications.* SIAM Rev. 51(3) (2009) 455–500.

[35] K.N. Kudin, and G.E. Scuseria, *Revisiting infinite lattice sums with the periodic Fast Multipole Method*, J. Chem. Phys. 121, 2886-2890 (2004).

[36] M. Lorenz, D. Usvyat, and M. Schütz. *Local ab initio methods for calculating optical band gaps in periodic systems. I. Periodic density fitted local configuration interaction singles method for polymers.* J. Chem. Phys. **134**, 094101 (2011); doi: 10.1063/1.3554209.

[37] S. A. Losilla, D. Sundholm, J. Juselius. *The direct approach to gravitation and electrostatics method for periodic systems.* J. Chem. Phys. 132 (2) (2010) 024102.

[38] M. Luskin, C. Ortner, and B. Van Koten. *Formulation and optimization of the energy-based blended quasicontinuum method.* Comput. Methods Appl. Mech. Engrg., 253, 2013.

[39] C. Pisani, M. Schütz, S. Casassa, D. Usvyat, L. Maschio, M. Lorenz, and A. Erba. *CRYSCOR: a program for the post-Hartree-Fock treatment of periodic systems.* Phys. Chem. Chem. Phys., 2012, **14**, 7615-7628.

[40] E.L. Pollock, and Jim Glosli. *Comments on P^3M, FMM, and the Ewald method for large periodic Coulombic systems.* Computer Phys. Communication **95** (1996), 93-110.

[41] F. Stenger. *Numerical methods based on Sinc and analytic functions.* Springer-Verlag, 1993.

[42] A.Y. Toukmaji, and J. Board Jr. *Ewald summation techniques in perspective: a survey.* Computer Phys. Communication **95** (1996), 73-92.

[43] Elena Voloshina, Denis Usvyat, Martin Schütz, Yuriy Dedkov and Beate Paulus. *On the physisorption of water on graphene: a CCSD(T) study.* Phys. Chem. Chem. Phys., 2011, 13, 12041-12047.

[44] O.V. Yazyev, E.N. Brothers, K.N. Kudin, and G.E. Scuseria, *A finite temperature linear tetrahedron method for electronic structure calculations of periodic systems*, J. Chem. Phys. 121, 2466-2470 (2004).

[45] E. Zeidler. *Oxford User's Guide to Mathematics.* Oxford University Press, 2003.